P_1-NONCONFORMING FINITE ELEMENTS ON TRIANGULATIONS INTO TRIANGLES AND QUADRILATERALS*

R. ALTMANN† AND C. CARSTENSEN‡

Abstract. The P_1-nonconforming finite element is introduced for arbitrary triangulations into quadrilaterals and triangles of multiple connected Lipschitz domains. An explicit a priori analysis for the combination of the Park–Sheen and the Crouzeix–Raviart nonconforming finite element methods is given for second-order elliptic PDEs with inhomogeneous Dirichlet boundary conditions.

Key words. nonconforming finite elements, elliptic problems, a priori estimates

AMS subject classifications. 65N30, 65N12, 65N15

DOI. 10.1137/110823675

1. Introduction. Park and Sheen [PS03, Par03] introduced a basis for nonconforming P_1 finite elements on triangulations into quadrilaterals of simply connected domains. Adaptive mesh-refinement has recently been proved to be optimal for the related Crouzeix–Raviart nonconforming FEM on triangles [BM08, Rab10]. In order to use adaptive mesh-refinements with the Park–Sheen nonconforming FEM on quadrilaterals, this paper introduces the combination of Park–Sheen with Crouzeix–Raviart nonconforming finite elements. This requires understanding the Park–Sheen FEM on multiple connected domains which consist of the domain Ω without all triangles. The first main result of this paper characterizes a basis of this nonconforming finite element space with global *edge-connected exceptional* basis functions of Definition 2.5, below. The second main result is a complete a priori error analysis with explicit constants for smooth solutions of second-order elliptic boundary value problems with inhomogeneous Dirichlet conditions. For the Poisson model problem

$$(1.1) \qquad -\Delta u = f \text{ in } \Omega := (0,1)^2 \text{ and } u = 0 \text{ on } \partial\Omega$$

and a uniform triangulation of Ω into squares and right isosceles triangles of size h, the a priori estimate of this paper implies for the energy norm (cf. Remark 5.2 below for a proof)

$$\||u - u_{PS}\||_{NC} \le 1.75h \, \|f\|_{L^2(\Omega)}.$$

The proposed combination of the Park–Sheen and the Crouzeix–Raviart nonconforming elements combines the minimal degrees of freedom per element domain with the flexibility of adaptive mesh-refinements. The rest of the paper is organized as follows. Section 2 introduces a basis of the nonconforming and piecewise linear finite

---

†Institut für Mathematik, Technische Universität Berlin, Straße des 17. Juni 136, D-10623 Berlin Charlottenburg, Germany (raltmann@math.tu-berlin.de). This author's work was supported by the Berlin Mathematical School, the KKGS Stiftung, the Humboldt-Universität zu Berlin, and the ERC grant "Modeling, Simulation and Control of Multi-Physics Systems."

‡Institut für Mathematik, Humboldt–Universität zu Berlin, Unter den Linden 6, D-10099 Berlin, Germany, and Department of Computational Science and Engineering, Yonsei University, 120-749 Seoul, Korea (cc@math.hu-berlin.de).

element space on triangulations into triangles and quadrilaterals. Section 3 discusses inhomogeneous Dirichlet boundary data and the possibility of inconsistent boundary conditions. Section 4 analyzes a nonconforming interpolation operator, which ensures consistent boundary data. Section 5 presents explicit constants for an a priori estimate for second-order elliptic PDEs. The numerical experiment of the Poisson problem on a Z-shape with graded meshes and combined triangles and quadrilaterals concludes the paper and underlines the necessity of the flexible mixture of triangles and quadrilaterals.

We employ standard notation on Lebesgue and Sobolev spaces and write $a \lesssim b$ to abbreviate $a \leq cb$ with some constant c, independent of the mesh-size.

2. The P_1-nonconforming finite element. This section introduces a basis for nonconforming P_1 finite elements on triangulations into triangles and convex quadrilaterals. Let $\mathcal{T}$ be a regular triangulation (see [Cia78]) of the two-dimensional bounded and connected Lipschitz domain $\Omega \subset \mathbb{R}^2$ with polygonal boundary $\partial\Omega$ into closed triangles (namely, $\mathcal{T}^3$) and closed, convex quadrilaterals (namely, $\mathcal{T}^4$) with the set of edges $\mathcal{E}$ and the set of nodes $\mathcal{N}$. Here, regular means that hanging nodes are excluded in the sense that two distinct nondisjoint element domains share either a common edge or a common vertex. The first goal of this paper is a characterization of a basis of the nonconforming finite element space

$$PS(\mathcal{T}) := P_1(\mathcal{T}) \cap C(\{\mathrm{mid}(E) \mid E \in \mathcal{E}\})$$

of piecewise affine functions which are continuous at the midpoints of all interior edges. This generalizes the Crouzeix–Raviart finite elements $CR(\mathcal{T}^3)$ [CR73] as well as the nonconforming $P1$ finite elements on quadrilaterals after Park and Sheen [PS03] in the sense that they may be mixed arbitrarily.

Here and throughout this paper, $P_k(\mathcal{T})$ denotes the set of piecewise polynomials of degree $\leq k$ with respect to $\mathcal{T}$. Furthermore, $\mathrm{mid}(E)$ stands for the midpoint of the edge E, $N := |\mathcal{N}|$ denotes the number of nodes, and $\mathcal{N}(E)$ denotes the two endpoints of an edge E. All quadrilaterals in this paper are closed and convex with inner angles strictly smaller than π. All domains have polygonal boundary.

DEFINITION 2.1 (edge-neighbors, $\mathcal{R}_k$-related, edge-connected). *Two distinct element domains $A, B \in \mathcal{T}$ are edge-neighbors or $\mathcal{R}$-related if they share a common edge, written $A\mathcal{R}B$. Two element domains $A, B \in \mathcal{T}$ are $\mathcal{R}_k$-related, $k \geq 2$, if $A\mathcal{R}B$ or there exist $C_1, \ldots, C_m \in \mathcal{T}$ with $A\mathcal{R}C_1, C_1\mathcal{R}C_2, \ldots, C_m\mathcal{R}B$ and $m \leq k-1 \in \mathbb{N} \cup \{\infty\}$. Two element domains A and B in $\mathcal{T}$ are called edge-connected if $A\mathcal{R}_\infty B$.*

Remark 2.1. The relation $\mathcal{R}_\infty$ is an equivalence relation and defines equivalence classes called edge-connectivity components.

DEFINITION 2.2 (nodal basis function I). *Given an edge-connected triangulation $\mathcal{T}^4$ of a Lipschitz domain into quadrilaterals with set of edges $\mathcal{E}(z) := \{E \in \mathcal{E} \mid z \in \mathcal{N}(E)\}$ and the respective set of midpoints $\mathrm{mid}(\mathcal{E}(z))$, a nodal basis function $\varphi_j \in PS(\mathcal{T}^4)$ is uniquely defined for every vertex z_j by*

(2.1)
$$\varphi_j(m) = \begin{cases} 1 & \text{if } m \in \mathrm{mid}(\mathcal{E}(z_j)), \\ 0 & \text{if } m \in \mathrm{mid}(\mathcal{E}) \setminus \mathrm{mid}(\mathcal{E}(z_j)). \end{cases}$$

Remark 2.2. (a) Any function $u \in P_1(Q)$ is characterized by the quadrilateral condition (diagonal rule) $m_1 + m_3 = m_2 + m_4$ for its values $m_1 = u(\mathrm{mid}(E_1)), \ldots, m_4 = u(\mathrm{mid}(E_4))$ at the consecutive midpoints $\mathrm{mid}(E_1), \ldots, \mathrm{mid}(E_4)$; see Figure 2.1. In particular, (2.1) is well defined in $PS(\mathcal{T}^4)$.
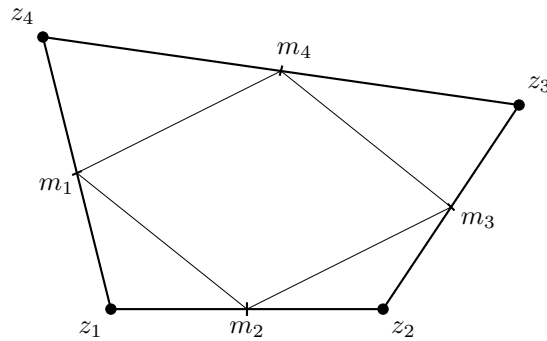
FIG. 2.1. *Diagonal rule $m_1 + m_3 = m_2 + m_4$ illustrates that the midpoints of a convex quadrilateral Q form a parallelogram.*

(b) For an enumeration $\mathcal{E} = \{E_1, \ldots, E_{|\mathcal{E}|}\}$, any $u \in PS(\mathcal{T}^4)$ is represented by the vector $x_u \in \mathbb{R}^{|\mathcal{E}|}$ defined by

$$x_u(j) := u(\mathrm{mid}(E_j)), \ j = 1, \ldots, |\mathcal{E}|.$$

This stores the function values at the $|\mathcal{E}|$ midpoints of edges where u is continuous. Let $E_{j_1}, E_{j_2}, E_{j_3}, E_{j_4}$ denote the consequent edges of the quadrilateral Q_j and let the matrix $M \in \{-1, 0, 1\}^{|\mathcal{T}^4| \times |\mathcal{E}|}$ equal

$$M_{jk} = \begin{cases} 1 & \text{if } k = j_1 \text{ or } k = j_3, \\ -1 & \text{if } k = j_2 \text{ or } k = j_4, \\ 0 & \text{otherwise} \end{cases}$$

for $j = 1, \ldots, |\mathcal{T}^4|$, $k = 1, \ldots, |\mathcal{E}|$, which represents all $|\mathcal{T}^4|$ diagonal rules. Then, $u \in PS(\mathcal{T}^4)$ implies $M x_u = 0$. In addition, for a continuous function v with coefficient vector x_v defined as above, $M x_v = 0$ implies the unique existence of a function $v_{PS} \in PS(\mathcal{T}^4)$ with $v(\mathrm{mid}(E_j)) = v_{PS}(\mathrm{mid}(E_j))$ for $j = 1, \ldots, |\mathcal{E}|$.

THEOREM 2.1 (see [PS03]). *Let $\mathcal{T}^4$ be an edge-connected regular triangulation of the simply connected Lipschitz domain $\Omega \subset \mathbb{R}^2$ into quadrilaterals with edges $\mathcal{E}$ and nodes $\mathcal{N}$. Then $PS(\mathcal{T}^4)$ has the dimension $|\mathcal{E}| - |\mathcal{T}^4| = N - 1$ with the counting measure $|\cdot|$ such that $|\mathcal{E}|$, $N := |\mathcal{N}|$, $|\mathcal{T}^4|$ denote the number of edges, nodes, and quadrilaterals. For any $j_0 \in \{1, \ldots, N\}$, with the omission operator $\overset{\vee}{\cdot}$,*

$$(\varphi_1, \ldots, \overset{\vee}{\varphi}_{j_0}, \ldots, \varphi_N) := (\varphi_1, \ldots, \varphi_{j_0-1}, \varphi_{j_0+1}, \ldots, \varphi_N)$$

is a basis of $PS(\mathcal{T}^4)$.

DEFINITION 2.3 (multiple connected). *A bounded, connected, and open set $\Omega \subset \mathbb{R}^2$ is called k-times connected if there exist exactly k connectivity components of $\partial\Omega = \Gamma_0 \cup \Gamma_1 \cup \cdots \cup \Gamma_{k-1}$, where $\Gamma_0, \ldots, \Gamma_{k-1}$ are pairwise disjoint connected compact sets in $\mathbb{R}^2$ such that Γ_0 is the boundary of the unbounded connectivity component of $\mathbb{R}^2 \setminus \Omega$.*

Although we are interested in Lipschitz domains we have to consider non-Lipschitz domains for quadrilaterals. The reason is that in the combination of triangles and quadrilaterals every edge-connectivity component of quadrilaterals will be discussed separately, which could be possibly non-Lipschitz. An example is the triangulation
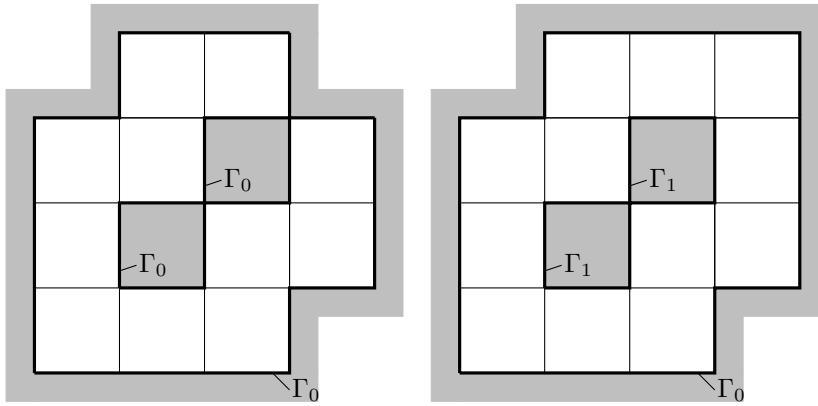
FIG. 2.2. *Example of (left) a simply and (right) a twice connected non-Lipschitz domain.*
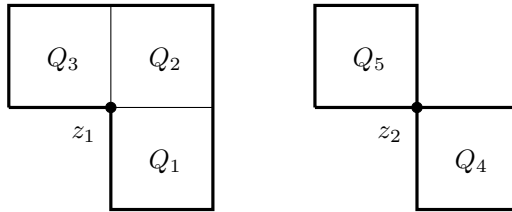

FIG. 2.3. *Examples of M_n edge-connectivity components of $\mathcal{T}^4(z_n)$: (left) $\mathcal{T}^4(z_1) = \mathcal{C}_{1,1} = \{Q_1, Q_2, Q_3\}$ for $M_1 = 1$ and (right) $\mathcal{T}^4(z_2) = \mathcal{C}_{2,1} \dot\cup \mathcal{C}_{2,2}$ with $\mathcal{C}_{2,1} = \{Q_4\}$, $\mathcal{C}_{2,2} = \{Q_5\}$ for $M_2 = 2$.*

from Figure 2.2, where the holes are filled with two triangles, respectively. For arbitrary connected polygonal domains we have to allow, in contrast to Lipschitz domains, multiple nodal basis functions per node. For any node $z_n \in \mathcal{N}$ the neighboring quadrilaterals

$$\mathcal{T}^4(z_n) := \{Q \in \mathcal{T}^4 | z_n \in \mathcal{N}(Q)\}$$

are partitioned into M_n pairwise disjoint edge-connectivity components $\mathcal{C}_{n,1}, \ldots, \mathcal{C}_{n,M_n}$,

$$\mathcal{T}^4(z_n) = \mathcal{C}_{n,1} \dot\cup \mathcal{C}_{n,2} \dot\cup \ldots \dot\cup \mathcal{C}_{n,M_n}.$$

For an example see Figure 2.3. Notice that for Lipschitz domains $M_1 = M_2 = \cdots = M_N = 1$ holds.

DEFINITION 2.4 (nodal basis function II). *For any node z_n with neighboring quadrilaterals $\mathcal{T}^4(z_n) = \mathcal{C}_{n,1} \dot\cup \ldots \dot\cup \mathcal{C}_{n,M_n}$ we define M_n nodal basis functions $\varphi_{n,1}, \ldots, \varphi_{n,M_n} \in PS(\mathcal{T}^4)$ in the following way. Given a triangulation $\mathcal{C}_{n,m}$, define $\varphi \in PS(\mathcal{C}_{n,m})$ as in Definition 2.2 and extend φ by zero to a function $\varphi_{n,m}$ in $PS(\mathcal{T}^4)$.*

The rest of this section is devoted to multiple connected domains. Figure 2.4 illustrates that the nodal basis functions from Definition 2.4 do not suffice.

Example 2.1 (necessity of new basis functions). The triangulation $\mathcal{T}^4$ of the domain $\Omega = (-1, 2)^2 \setminus [0, 1]^2$ into eight squares of size 1 as in Figure 2.4 displays (left) nodal basis functions $-\varphi_1, +\varphi_2, \ldots, +\varphi_{16}$ of the type defined in Definition 2.2. In fact, one can prove that $\varphi_1, \ldots, \varphi_{15}$ are linearly independent, whence dim $PS(\mathcal{T}^4) \geq 15$.
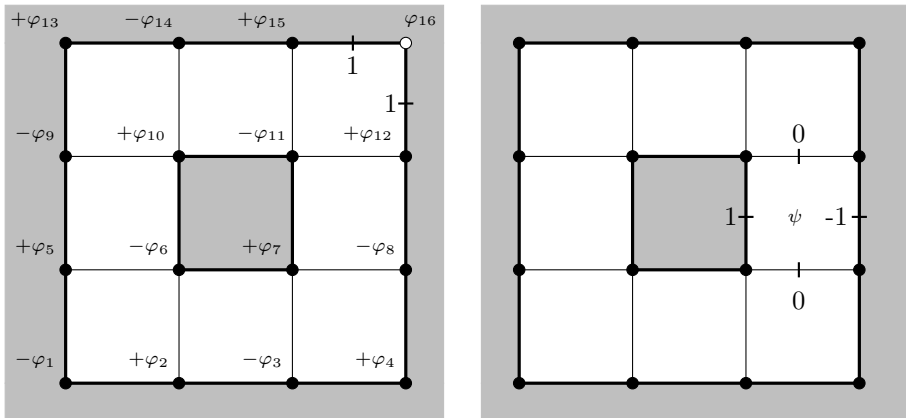
FIG. 2.4. *Nodal basis functions $\varphi_1, \ldots, \varphi_{16}$ from Definition* 2.2 *(left) are linearly dependent and (right) exclude $\psi \in PS(\mathcal{T}^4)$ as discussed in Example* 2.1.

Since $\varphi_{16} = -\varphi_1 + \varphi_2 - \cdots - \varphi_{14} + \varphi_{15}$, φ_{16} lies in span$\{\varphi_1, \ldots, \varphi_{15}\}$. The right side of Figure 2.4 displays

$$\psi \in PS(\mathcal{T}^4) \setminus \text{span}\{\varphi_1, \ldots, \varphi_{15}\}$$

and hence dim $PS(\mathcal{T}^4) \geq 16$. An immediate proof of $\psi \notin \text{span}\{\varphi_1, \ldots, \varphi_{15}\}$ employs the linear functional

$$\ell : PS(\mathcal{T}^4) \to \mathbb{R}, \quad v \mapsto v(1/2, 0) + v(1/2, 1) - v(0, 1/2) - v(1, 1/2)$$

and the fact $\ell(\varphi_1) = \cdots = \ell(\varphi_{15}) = 0 \neq 1 = \ell(\psi)$.

Example 2.1 suggests enlarging the set of nodal basis functions by some other functions in $PS(\mathcal{T}^4)$ which somehow link connectivity components of $\mathbb{R}^2 \setminus \Omega$. In what follows $\mathcal{E}(D)$ denotes the set of edges in the subset $D \subseteq \overline{\Omega}$.

DEFINITION 2.5 (edge-path). *Let $\mathcal{T}^4$ be an edge-connected triangulation into quadrilaterals of some k-times connected domain $\Omega \subset \mathbb{R}^2$ with $k \geq 2$. Further let Γ_a and Γ_b denote two different components of $\partial\Omega$. Choose a subtriangulation $\{Q_1, \ldots, Q_J\} \subset \mathcal{T}^4$ which is (in itself) edge-connected and satisfies*

$$\mathcal{E}(Q_1) \cap \mathcal{E}(\Gamma_a) \neq \emptyset \quad and \quad \mathcal{E}(Q_J) \cap \mathcal{E}(\Gamma_b) \neq \emptyset$$

as well as

$$E_{j+1} := \mathcal{E}(Q_j) \cap \mathcal{E}(Q_{j+1}) \in \mathcal{E} \text{ for } j = 1, \ldots, J - 1.$$

Then, for any choice

$$E_1 \in \mathcal{E}(Q_1) \cap \mathcal{E}(\Gamma_a) \quad and \quad E_{J+1} \in \mathcal{E}(Q_J) \cap \mathcal{E}(\Gamma_b),$$

an edge-path $\psi \in PS(\mathcal{T}^4)$ is defined by

$$(2.2) \qquad \psi(m) := \begin{cases} 1 & \text{if } m = \text{mid}(E_1), \\ \pm 1 & \text{if } m = \text{mid}(E_j) \text{ for } j = 2, \ldots, J, \\ 0 & \text{for any other midpoint.} \end{cases}$$

FIG. 2.5. *Illustration of ψ from Definition 2.5. Since $\mathcal{E}(Q_1) \cap \mathcal{E}(\Gamma_a)$ allows two choices of E_1, there exists a second choice of ψ.*

For $j = 1, \ldots, J - 1$ *the signs are uniquely defined by* $\psi(\mathrm{mid}(E_{j+1})) = \psi(\mathrm{mid}(E_j))$ *if* $E_j \cap E_{j+1} \neq \emptyset$ *and* $\psi(\mathrm{mid}(E_{j+1})) = -\psi(\mathrm{mid}(E_j))$ *if* $E_j \cap E_{j+1} = \emptyset$.

Remark 2.3. (a) It holds that $\mathrm{supp}\,\psi = Q_1 \cup \cdots \cup Q_J$.

(b) The choice of E_1 and E_J is not unique; cf. Figure 2.5. Also, the subtriangulation $\{Q_1, \ldots, Q_J\}$ and therefore $\mathrm{supp}\,\psi$ is not unique; cf. Figure 2.4. Thus, there exist several possibilities for ψ.

The following theorem introduces a basis of $PS(\mathcal{T}^4)$ for general multiple connected domains with polygonal boundary.

THEOREM 2.2 (basis for multiple connected domains). *For the regular triangulation $\mathcal{T}^4$ of the k-times connected domain $\Omega \subset \mathbb{R}^2$ into edge-connected quadrilaterals, $PS(\mathcal{T}^4)$ has the k-independent dimension*

$$\dim(PS(\mathcal{T}^4)) = |\mathcal{E}| - |\mathcal{T}^4|.$$

Let $\varphi_{n,m}$ denote the nodal basis functions for $n = 1, \ldots, N$, $m = 1, \ldots, M_n$ from Definition 2.4. Further, let $\psi_1, \ldots, \psi_{k-1}$ denote edge-paths from Definition 2.5, each connecting two pairwise disjoint connectivity components of $\partial\Omega$ such that each connectivity component of $\partial\Omega$ appears at least once. Then, for any (n_0, m_0), $n_0 \in \{1, \ldots, N\}$, $m_0 \in \{1, \ldots, M_{n_0}\}$,

$$(2.3) \qquad (\psi_1, \ldots, \psi_{k-1}, \varphi_{1,1}, \ldots, \varphi_{1,M_1}, \varphi_{2,1}, \ldots, \overset{\vee}{\varphi}_{n_0,m_0}, \ldots, \varphi_{N,M_N})$$

(with the omission operator $\overset{\vee}{\cdot}$) is a basis of $PS(\mathcal{T}^4)$.

Proof. The arguments in the proof of $\dim(PS(\mathcal{T}^4)) \leq |\mathcal{E}| - |\mathcal{T}^4|$ in [PS03, p. 632] work identically for multiple connected domains. It remains to show that (2.3) are $|\mathcal{E}| - |\mathcal{T}^4|$ linearly independent functions in order to prove that this defines a basis.

The proof uses mathematical induction over the number of quadrilaterals in $\mathcal{T}^4$. The initial step $|\mathcal{T}^4| = 1$, i.e., a triangulation of only one quadrilateral which is simply connected and Lipschitz, is already shown by Theorem 2.1. Assume that the claim is true for triangulations into n quadrilaterals and let $\mathcal{T}^4$ be an arbitrary triangulation into $n + 1 \geq 2$ edge-connected quadrilaterals. Choose a quadrilateral $Q \in \mathcal{T}^4$ which contains a boundary edge such that $\mathcal{S}^4 := \mathcal{T}^4 \setminus \{Q\}$ still is edge-connected. The induction hypothesis gives a basis for $PS(\mathcal{S}^4)$. We distinguish four cases.

Case 1. $|\mathcal{E}(Q) \cap \mathcal{E}(\mathcal{S}^4)| = 1$ (cf. Figure 2.6). First, we consider all basis functions of $PS(\mathcal{S}^4)$ which vanish in M_1. Those functions can be extended by zero to functions in $PS(\mathcal{T}^4)$. Second, basis functions with nonzero values in M_1 are extended by the same

FIG. 2.6. *Situation of (left) Case* 1 *and (right) Case* 2 *in the proof of Theorem* 2.2.
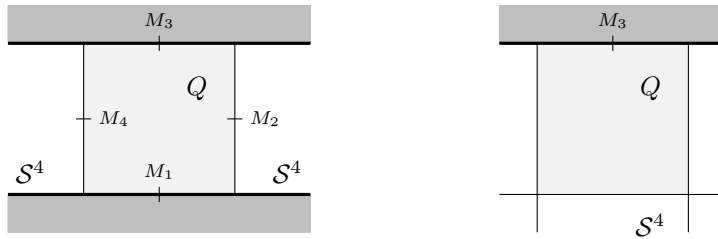

FIG. 2.7. *Situation of (left) Case* 3 *and (right) Case* 4 *in the proof of Theorem* 2.2.

value in M_4 and zero elsewhere such that the quadrilateral condition of Q is fulfilled. All these functions are still linearly independent in $PS(\mathcal{T}^4)$. Together with the nodal basis functions from Definition 2.4 at A and B, which are obviously independent because of their value in M_3, we constructed

$$(|\mathcal{E}| - 3) - |\mathcal{S}^4| + 2 = (|\mathcal{E}| - 3) - (|\mathcal{T}^4| - 1) + 2 = |\mathcal{E}| - |\mathcal{T}^4|$$

independent functions.

Case 2. $\mathcal{E}(Q) \cap \mathcal{E}(\mathcal{S}^4)$ are exactly two neighboring edges (cf. Figure 2.6). Again we extend all basis functions of $PS(\mathcal{S}^4)$ to $PS(\mathcal{T}^4)$ by zero if they vanish in M_1 and M_2. Otherwise we extend with zero in M_3 and the appropriate value in M_4 such that the diagonal rule in Q is fulfilled. With the same argumentation as above, these are together with the nodal basis function from Definition 2.4 at A

$$(|\mathcal{E}| - 2) - (|\mathcal{T}^4| - 1) + 1 = |\mathcal{E}| - |\mathcal{T}^4|$$

linearly independent functions.

Case 3. $\mathcal{E}(Q) \cap \mathcal{E}(\mathcal{S}^4)$ are exactly two opposed edges (cf. Figure 2.7). In this case we extend all basis functions of $PS(\mathcal{S}^4)$ with zero in M_1 and with some value in M_3 such that the quadrilateral condition of Q is fulfilled. Here, we have to add an edge-path from Definition 2.5, i.e., the function which has the values 1 in M_1, -1 in M_3, and zero in all other midpoints. This ensures with the induction hypothesis that all connectivity components of $\partial\Omega$ are linked by edge-paths. Obviously, these are $|\mathcal{E}| - |\mathcal{T}^4|$ linearly independent functions.

Case 4. $|\mathcal{E}(Q) \cap \mathcal{E}(\mathcal{S}^4)| = 3$ (cf. Figure 2.7). Since $(|\mathcal{E}| - 1) - |\mathcal{S}^4| = |\mathcal{E}| - |\mathcal{T}^4|$, we just have to extend all basis functions of $PS(\mathcal{S}^4)$ by the appropriate value in M_3 (quadrilateral condition).

At this state, we have found a basis of $PS(\mathcal{T}^4)$ which does not totally coincide with (2.3). However, the choice of the basis of $PS(\mathcal{S}^4)$ and some easy linear combinations (especially with the new added functions) yield the claim.   □

Remark 2.4. Let B be the $(|\mathcal{E}| - |\mathcal{T}^4|) \times |\mathcal{E}|$ matrix, where $B(f,e)$ gives the value of the fth function in (2.3) at the midpoint of the eth edge and M the matrix from Remark 2.2(b) which stores all quadrilateral conditions. Then the theorem says that a vector x satisfies $Mx = 0$ if and only if x is a linear combination of the rows of B. Therein the vector x contains the function values of a function in $PS(\mathcal{T}^4)$ at the $|\mathcal{E}|$ midpoints of edges.

THEOREM 2.3 (basis of PS($\mathcal{T}$)). *Let $\mathcal{T} = \mathcal{T}^3 \cup \mathcal{T}^4$ be a regular triangulation of the bounded Lipschitz domain Ω into triangles and quadrilaterals.*

Furthermore, $\mathcal{T}^4 = \mathcal{C}_1 \dot\cup \mathcal{C}_2 \dot\cup \ldots \dot\cup \mathcal{C}_K$, where each $\mathcal{C}_k$ denotes one edge-connectivity component of $\mathcal{T}^4$. Let $\mathcal{B}_k = (f_{k,1}, \ldots, f_{k,|\mathcal{B}_k|})$ denote a basis of $PS(\mathcal{C}_k)$ for each $k = 1, \ldots, K$, according to Theorem 2.2. By $F_{k,j} \in PS(\mathcal{T})$ we denote the extension of $f_{k,j}$ by zero at all midpoints of $\mathcal{E} \setminus \mathcal{E}(\mathcal{C}_k)$, $k = 1, \ldots, K$, $j = 1, \ldots, |\mathcal{B}_k|$. Further let ϕ_E denote the Crouzeix–Raviart basis function for any edge E which is not part of a quadrilateral. The function ϕ_E has the value 1 at the midpoint of E and is zero at all midpoints of $\mathcal{E} \setminus \{E\}$. Then, with the enumeration $\mathcal{E}(\mathcal{T}^3) \setminus \mathcal{E}(\mathcal{T}^4) = \{E_1, \ldots, E_L\}$,

$$(2.4) \qquad (F_{1,1}, \ldots, F_{1,|\mathcal{B}_1|}, F_{2,1}, \ldots, F_{K,|\mathcal{B}_K|}, \phi_{E_1}, \ldots, \phi_{E_L})$$

is a basis of $PS(\mathcal{T})$ and $\dim(PS(\mathcal{T})) = |\mathcal{E}| - |\mathcal{T}^4|$.

Proof. Consider a linear combination of functions in (2.4) which gives zero and therefore vanishes at all midpoints of $\mathcal{E}$. For $j = 1, \ldots, L$, the Crouzeix–Raviart basis function ϕ_{E_j} is the only function in (2.4) with $\phi_{E_j}(\mathrm{mid}(E_j)) \neq 0$. Thus the coefficients of $\phi_{E_1}, \ldots, \phi_{E_L}$ have to vanish. Since the components $\{\mathcal{C}_k\}$ cannot be edge-connected, we can consider each edge-connectivity component separately. The fact that $\mathcal{B}_k$ is a basis of $PS(\mathcal{C}_k)$ shows the linear independence of (2.4).

Given an arbitrary $u_{PS} \in PS(\mathcal{T})$, again we use the fact that $\mathcal{B}_k$ is a basis of $PS(\mathcal{C}_k)$. Consequently, the values of u_{PS} at the midpoints of $\mathcal{E}(\mathcal{T}^4)$ can be designed. For any remaining edge, i.e., $\mathcal{E}(\mathcal{T}^3) \setminus \mathcal{E}(\mathcal{T}^4)$, there exists a Crouzeix–Raviart basis function. ☐

3. Consistent boundary conditions. This section is devoted to Dirichlet boundary conditions and the concept of consistent Dirichlet data. In fact, the diagonal rule of $PS(Q)$ for a quadrilateral Q states a necessary condition for the values at the midpoints of $\mathcal{E}(Q)$.

DEFINITION 3.1 (consistent Dirichlet data). *Consider Dirichlet data given by the values at the midpoints of $\mathcal{E}(\Gamma_D)$. Such data are called* consistent *if there exists a linear combination of functions in $PS(\mathcal{T})$ which have the given boundary values at the midpoints of $\mathcal{E}(\Gamma_D)$.*

The following theorem shows how to recognize triangulations where inconsistent boundary data can appear.

THEOREM 3.1. *Let $\Gamma_0, \ldots, \Gamma_{k-1}$ denote the connectivity components of $\partial\Omega = \Gamma_D$ and $\mathcal{T}$ a triangulation into quadrilaterals and triangles. Then, every Dirichlet data is consistent if and only if there exists a component Γ_{j_0} which contains an edge of a triangle or consists of an odd quantity of edges.*

Proof. Consider that each boundary component consists only of quadrilateral edges and all quantities of edges are even. With $\mathcal{E}(\partial\Omega) = \{E_1, \ldots, E_{2k}\}$ we show that the data with 1 at the midpoint of $E_1 = \mathrm{conv}\{A, B\}$ and zero at midpoints of $\mathcal{E}(\partial\Omega) \setminus \{E\}$ are not consistent. Since edge-paths just shift boundary data to different boundary components, we can assume that Ω is simply connected. Thus, only φ_A and φ_B are nonzero at $\mathrm{mid}(E_1)$. To generate the value 1 we use x times φ_A. To reach all the zeros at the boundary one gets alternately minus and plus x times the

corresponding nodal basis function. Because of the even quantity of boundary edges, we obtain $-x$ times φ_B. Thus, the value on the midpoint of E_1 is $x - x = 0$, which is a contradiction.

For the other direction we construct the boundary data with the value 1 on an arbitrary boundary edge $E = \operatorname{conv}\{A, B\}$ and zero anywhere else. Because of the edge-paths, it suffices to consider edges of Γ_{j_0}. On edges of triangles there is nothing to show, hence we consider an edge of a quadrilateral. To construct the required boundary data, we set $1/2$ times φ_A and $1/2$ times φ_B. To obtain all the zero values, we set alternately minus and plus $1/2$ times the corresponding nodal basis function. This algorithm works because of the odd quantity of edges or stops if an edge of a triangle appears.   □

Remark 3.1. Consistent boundary conditions are necessary for the existence of discrete solutions in section 5.1. Theorem 5.2 presents sufficient conditions as well.

Remark 3.2. In the case of inconsistent data one may change the triangulation, i.e., split one quadrilateral at the boundary into two triangles; see Theorem 3.1. One may also change the data and consider the projection $\mathbf{b}_D^{con}$ of the boundary data $\mathbf{b}_D$ into the space of consistent boundary.

The approximation operator of the next section will lead to consistent boundary data.

4. Approximation operator J. This section analyzes the nonconforming interpolation operator for triangulations into triangles and quadrilaterals and serves as preparation for the calculation of explicit a priori constants in section 5.

DEFINITION 4.1 (approximation operator J [PS03]). *We define the* approximation operator $J : C(\overline{\Omega}) \to PS(\mathcal{T})$ *by*

$$(J\varphi)(m) := \frac{1}{2}(\varphi(P_1) + \varphi(P_2)) \;\; for \;\; m = (P_1 + P_2)/2 \in \operatorname{mid}(\mathcal{E})$$

for all midpoints $m \in \operatorname{mid}(\mathcal{E})$, $P_1, P_2 \in \mathcal{N}$ *with* $\operatorname{conv}\{P_1, P_2\} \in \mathcal{E}$ *and* $\varphi \in C(\overline{\Omega})$.

Remark 4.1. Since J maps into $PS(\mathcal{T})$, the operator designs consistent boundary data for given Dirichlet data $u_D \in C(\overline{\Omega})$.

PROPOSITION 4.1. *Let* $T = \operatorname{conv}\{P_1, P_2, P_3\}$ *be a triangle with greatest interior angle* α, *diameter* h_T, *and*

$$C(\alpha) := \left(\frac{1/4 + 2/\pi^2}{1 - |\cos \alpha|} \right)^{1/2}.$$

Then, for $w \in H^2(T)$ *and the nodal interpolation operator* I_C, *it holds that*

$$(4.1) \qquad \|\nabla(w - I_C w)\|_{L^2(T)} \le C(\alpha) h_T \|D^2 w\|_{L^2(T)},$$

$$(4.2) \qquad \|w - I_C w\|_{L^2(T)} \le \sqrt{5/3}\, C(\alpha) h_T^2 \|D^2 w\|_{L^2(T)}.$$

Proof. The proof of (4.1) can be found in [CGR11]. With mean integral $\fint \cdot\, dx$, one notices the trace identity

$$(4.3) \qquad \fint_E f\, ds = \fint_T f\, dx + \frac{1}{2} \fint_T (x - P) \cdot \nabla f(x)\, dx$$

follows if $T = \operatorname{conv}\{E, P\}$, $E \in \mathcal{E}(T)$, $P \in \mathcal{N}(T)$ with integration by parts and

elementary geometry. Set $e := w - I_C w$ and obtain by the trace identity ($f = e^2$)

$$\|e\|_{L^2(T)}^2 \leq \frac{|T|}{|E|}\|e\|_{L^2(E)}^2 + h_T\|e\|_{L^2(T)}\|\nabla e\|_{L^2(T)}$$

$$\leq \frac{|T|}{|E|}\|e\|_{L^2(E)}^2 + \frac{1}{2}\|e\|_{L^2(T)}^2 + \frac{h_T^2}{2}\|\nabla e\|_{L^2(T)}^2.$$

Since e vanishes at the endpoints of E, we use the Friedrichs inequality. In addition, we again use the trace identity with $f = |\partial e/\partial s|^2$, which gives

$$\frac{|T|}{|E|}\|e\|_{L^2(E)}^2 \leq \frac{|T||E|}{\pi^2}\|\partial e/\partial s\|_{L^2(E)}^2 \leq \frac{h_T^2}{\pi^2}\|\nabla e\|_{L^2(T)}^2 + \frac{h_T^3}{\pi^2}\|\nabla e\|_{L^2(T)}\|D^2 e\|_{L^2(T)}.$$

The aforementioned estimates and the first claim (4.1) lead with $2/\pi \leq C(\alpha)$ eventually to

$$\frac{1}{2}\|e\|_{L^2(T)}^2 \leq \frac{h_T^2}{\pi^2}\|\nabla e\|_{L^2(T)}^2 + \frac{h_T^3}{\pi^2}\|\nabla e\|_{L^2(T)}\|D^2 w\|_{L^2(T)} + \frac{h_T^2}{2}\|\nabla e\|_{L^2(T)}^2$$

$$\leq \frac{5C^2(\alpha)}{6}h_T^4 \|D^2 w\|_{L^2(T)}^2. \qquad \square$$

The a priori estimate requires an estimate for $\|w - Jw\|_{H^1(Q)}^2$ and some shape regularity conditions on the triangulation $\mathcal{T}$. Suppose that interior angles ω in $\mathcal{T}$ are uniformly bounded from below and bounded away from π in the sense of

$$0 < \omega_0 \leq \omega \leq \pi - \omega_0 < \pi$$

with some universal constant $\omega_0 > 0$. Let $\theta_0 > 0$ be the smallest angle of diagonals in all quadrilaterals in $\mathcal{T}$.

Remark 4.2. For a quadrilateral Q divided by a diagonal into two triangles, the largest interior angles of the triangles belong to the interval $[\omega_0, \pi - \omega_0]$. Hence,

(4.4) $$\|\nabla(w - I_C w)\|_{L^2(Q)} \leq C(\omega_0)h_Q\|D^2 w\|_{L^2(Q)}.$$

The rest of this section proves the following theorem.

THEOREM 4.2. *Let Q be a convex quadrilateral with constants $C(\theta_0)$ and $C(\omega_0)$ as defined in Proposition 4.1. Then, for any $w \in H^2(Q)$, it holds that*

(4.5) $$\|\nabla(w - Jw)\|_{L^2(Q)} \leq C(\theta_0)h_Q\|D^2 w\|_{L^2(Q)},$$

(4.6) $$\|w - Jw\|_{L^2(Q)} \leq (2C(\omega_0) + C(\theta_0)/2)h_Q^2\|D^2 w\|_{L^2(Q)}.$$

Proof. Let $E = \text{conv}\{P_1, P_3\}$ be one diagonal of $Q = \text{conv}\{P_1, \ldots, P_4\}$ with unit tangent vector $\tau := (P_3 - P_1)/|P_3 - P_1|$. Let m_1 and m_2 be the edge midpoints of $\text{conv}\{P_1, P_2\}$ and $\text{conv}\{P_2, P_3\}$; see Figure 4.1. Then,

$$Jw(P_3) - Jw(P_1) = 2Jw(m_2) - 2Jw(m_1) = w(P_3) - w(P_1).$$

Hence $f := \nabla(w - Jw) \cdot \tau$ satisfies $\fint_E f\,ds = 0$. The trace identity (4.3) on $T_1 = \text{conv}\{P_2, E\}$ leads for $\bar{f} := \fint_{T_1} f\,dx$ to

$$|\bar{f}| \leq \frac{1}{2|T_1|}\|x - P_2\|_{L^2(T_1)}\|\nabla f\|_{L^2(T_1)} \leq \frac{h_T}{\sqrt{8|T_1|}}\|\nabla f\|_{L^2(T_1)}.$$
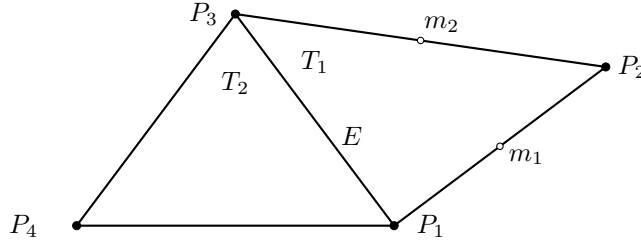
FIG. 4.1. *Quadrilateral Q divided by diagonal E into triangles T_1 and T_2 in the proof of Theorem* 4.2.

The Pythagoras theorem and the Poincaré inequality with the Payne–Weinberger constant [PW60] imply

$$(4.7) \qquad \|f\|^2_{L^2(T_1)} = \|f - \bar{f}\|^2_{L^2(T_1)} + \|\bar{f}\|^2_{L^2(T_1)} \le h_T^2 \left(\frac{1}{\pi^2} + \frac{1}{8} \right) \|\nabla f\|^2_{L^2(T_1)}.$$

The same calculation for T_2 as well as on the triangles which occur by the division of Q by the other diagonal with tangent vector $\mu := (P_4 - P_2)/|P_4 - P_2|$. $|\tau \cdot \mu| = |\cos \theta_0|$ equals the angle of the diagonals and [CGR11] shows

$$|a|^2 \le \frac{(a \cdot \tau)^2 + (a \cdot \mu)^2}{1 - |\tau \cdot \mu|} \quad \text{for all } a \in \mathbb{R}^2.$$

This is evaluated for $a := \nabla(w - Jw)(x)$ and thereafter integrated over $x \in Q$. The estimate (4.7) for all the triangles then proves (4.5).

The proof of the second claim employs the nodal interpolation operator I_C from Proposition 4.1 on the triangles T_1 and T_2 of Figure 4.1. Since $e := I_C w - Jw \in P_1(T_1)$ vanishes along $\overline{m_1 m_2}$,

$$e(y) = e(x) + \nabla e|_{T_1} \cdot (y - x) = \nabla e|_{T_1} \cdot (y - x)$$

for all $y \in T_1$ and $x \in \overline{m_1 m_2}$. Therefore,

$$\|e\|^2_{L^2(T_1)} \le h_{T_1}^2/4 \, \|\nabla e\|^2_{L^2(T_1)}.$$

This and an analogue on T_2 lead to

$$\|e\|^2_{L^2(Q)} \le h_Q^2/4 \, \|\nabla e\|^2_{L^2(Q)}.$$

The triangle inequality and (4.5)–(4.4) imply

$$\|\nabla e\|_{L^2(Q)} \le \|\nabla(w - I_C w)\|_{L^2(Q)} + \|\nabla(w - Jw)\|_{L^2(Q)}$$
$$\le (C(\omega_0) + C(\theta_0)) h_Q \, \|D^2 w\|_{L^2(Q)}.$$

This and (4.2) result in

$$\|w - Jw\|_{L^2(Q)} \le \|w - I_C w\|_{L^2(Q)} + \|e\|_{L^2(Q)}$$
$$\le \sqrt{5/3} \, C(\omega_0) h_Q^2 \|D^2 w\|_{L^2(Q)} + 1/2 \, (C(\omega_0) + C(\theta_0)) h_Q^2 \|D^2 w\|_{L^2(Q)}$$
$$\le (2C(\omega_0) + C(\theta_0)/2) h_Q^2 \|D^2 w\|_{L^2(Q)}. \qquad \square$$

5. A priori error estimate for elliptic PDEs. This section analyzes explicitly the involved constant in the a priori error estimate using Park–Sheen elements. Therefore, the existence of a unique solution of the discrete Dirichlet problem is shown first.

5.1. Model problem and its discretization. For the bounded Lipschitz domain Ω, the right-hand side $f \in L^2(\Omega)$, and $u_D \in H^2(\Omega)$, the elliptic boundary value problem reads

$$(5.1) \qquad \begin{aligned} -\operatorname{div}(\mathbb{A}\nabla u) + \mathbf{b} \cdot \nabla u + \gamma u &= f &&\text{in } \Omega, \\ u &= u_D &&\text{on } \partial\Omega. \end{aligned}$$

Here and throughout this paper, the matrix $\mathbb{A} \in L^\infty(\Omega; \mathbb{R}^{2\times 2})$ is bounded, symmetric, and uniformly positive definite in the sense that there exist positive $\alpha_{\min}, \alpha_{\max}$ with

$$0 < \alpha_{\min}|\xi|^2 \le \xi^t \mathbb{A}(x)\xi \le \alpha_{\max}|\xi|^2 < \infty \text{ for all } \xi \in \mathbb{R}^2 \text{ and a.e. } x \in \Omega.$$

Furthermore, let $\mathbf{b} \in H(\operatorname{div}, \Omega) \cap L^\infty(\Omega; \mathbb{R}^2)$ and $\gamma \in L^\infty(\Omega)$ be bounded almost everywhere by positive $\beta_{\max} := \|\mathbf{b}\|_{L^\infty(\Omega)}$ and $\gamma_{\max} := \|\gamma\|_{L^\infty(\Omega)}$ and assume

$$(5.2) \qquad \operatorname{div}\mathbf{b} \le 2\gamma \quad \text{a.e. in } \Omega.$$

The nonsymmetric bilinear form a with

$$a(u, v) := (\mathbb{A}\nabla u, \nabla v)_{L^2(\Omega)} + (\mathbf{b} \cdot \nabla u + \gamma u, v)_{L^2(\Omega)} \text{ for all } u, v \in H^1(\Omega)$$

is bounded and $H_0^1(\Omega)$-elliptic. With the linear functional $F := f - a(u_D, \cdot)$, the weak formulation reads as follows: seek $u_0 \in H_0^1(\Omega)$ such that

$$(5.3) \qquad a(u_0, v) = F(v) \text{ for any } v \in H_0^1(\Omega).$$

The Lax–Milgram lemma [BS08, p. 62] guarantees the unique existence of the weak solution $u := u_0 + u_D$. The regularity of u is a subtle issue and we refer to [Gri85] for sufficient conditions for $u \in H^2(\Omega)$.

Given a regular triangulation $\mathcal{T}$ of Ω into triangles and quadrilaterals, the finite element space with boundary conditions reads

$$PS_0(\mathcal{T}) = \{v_{PS} \in PS(\mathcal{T}) | \text{ for all } E \in \mathcal{E}(\partial\Omega), \ v_{PS}(\operatorname{mid}(E)) = 0\}.$$

The discrete problem involves the restriction of a to an element $Q \in \mathcal{T}$, namely,

$$a_Q(u, v) := (\mathbb{A}\nabla u, \nabla v)_{L^2(Q)} + (\mathbf{b} \cdot \nabla u + \gamma u, v)_{L^2(Q)},$$

and the discrete bilinear form

$$a_{NC}(u, v) := \sum_{Q \in \mathcal{T}} a_Q(u, v) \text{ for } u, v \in PS(\mathcal{T}) + H^1(\Omega).$$

The discrete bilinear form corresponds to

$$\|v\|_{NC} := a_{NC}(v, v)^{1/2} \text{ for } u, v \in PS(\mathcal{T}) + H^1(\Omega).$$

With $F_{NC} := f - a_{NC}(u_D, \cdot)$, the weak formulation for the discrete problem reads as follows: seek $u_{PS}^0 \in PS_0(\mathcal{T})$ such that

$$(5.4) \qquad a_{NC}(u_{PS}^0, v_{PS}) = F_{NC}(v_{PS}) \text{ for all } v_{PS} \in PS_0(\mathcal{T}).$$

Given any solution u_{PS}^0, the Park–Sheen approximation to the exact solution u reads $u_{PS} := u_{PS}^0 + Ju_D \in PS(\mathcal{T})$. The existence of the discrete solution is the subject of the next subsection.

5.2. Discrete ellipticity. The existence of a unique discrete solution is based on a discrete Friedrichs inequality for a partition $\mathcal{T}$ of Ω into triangles and quadrilaterals.

THEOREM 5.1 (discrete Friedrichs inequality). *There exists a constant C_{dF}, independent of the mesh-size of $\mathcal{T}$, such that any $v \in H_0^1(\Omega) + PS_0(\mathcal{T})$ satisfies*

$$(5.5) \qquad \|v\|_{L^2(\Omega)} \le C_{dF} \|\nabla_{NC} v\|_{L^2(\Omega)} := C_{dF} \left(\sum_{T \in \mathcal{T}} \|\nabla v\|_{L^2(T)}^2 \right)^{1/2}.$$

Proof. Let $\mathcal{T}^*$ be some refined triangulation into triangles where each quadrilateral in $\mathcal{T}$ is divided into two triangles. Then $v \in H_0^1(\Omega) + CR_0(\mathcal{T}^*)$ and (5.5) follows from [BS08, Theorem 10.6.12]. $\square$

Let κ denote the ratio of the largest and smallest edge in any quadrilateral, i.e.,

$$\max_{Q \in \mathcal{T}^4} \frac{\text{largest edge of } Q}{\text{smallest edge of } Q} =: \kappa.$$

If $\mathcal{T}$ consists only of triangles, set $\kappa = 1$.

THEOREM 5.2 (existence of a unique discrete solution). *Let $\mathbf{b} \in H(\text{div}, \Omega)$ be piecewise constant. For sufficient small mesh-size in the sense that*

$$(5.6) \qquad h_{\max} := \max\{h_T | \ T \in \mathcal{T}\} \le \frac{\alpha_{\min} \sin \omega_0}{2\kappa \beta_{\max}},$$

there exists a unique solution $u_{PS}^0 \in PS_0(\mathcal{T})$ of (5.4).

Proof. The boundedness of a_{NC} is obvious, so the focus is on the ellipticity with respect to the broken H^1-norm

$$\| \cdot \|_{H^1(\mathcal{T})} := (\| \cdot \|_{L^2(\Omega)}^2 + | \cdot |_{NC}^2)^{1/2} \ \text{ with } \ | \cdot |_{NC}^2 = \sum_{Q \in \mathcal{T}} \|\nabla \cdot \|_{L^2(Q)}^2.$$

Notice that $\mathbf{b} \in H(\text{div}, \Omega) \cap P_0(\mathcal{T}; \mathbb{R}^2)$ means that the jumps $[\mathbf{b} \cdot \nu_E]_E$ vanish across all interior edges. An elementwise integration by parts plus (5.2) lead to

$$\alpha_{\min} |u_{PS}^0|_{NC}^2 + \frac{1}{2} \sum_{Q \in \mathcal{T}} \int_{\partial Q} (\mathbf{b} \cdot \nu)(u_{PS}^0)^2 \ ds \le a_{NC}(u_{PS}^0, u_{PS}^0).$$

Let E be an edge of some quadrilateral Q. If E is an edge on the boundary $\partial \Omega$, u_{PS}^0 is affine and vanishes in $\text{mid}(E)$. It follows with $h_E^2/|Q| \le \kappa/\sin \omega_0$ that

$$\int_E (u_{PS}^0)^2 \ ds = \frac{h_E^3}{12} \left| \frac{\partial u_{PS}^0}{\partial s} \Big|_E \right|^2 \le \frac{h_E^3}{12|Q|} \|\nabla u_{PS}^0\|_{L^2(Q)}^2 \le \frac{h_E \kappa}{12 \sin \omega_0} \|\nabla u_{PS}^0\|_{L^2(Q)}^2.$$

For an interior edge $E = \mathcal{E}(Q_1) \cap \mathcal{E}(Q_2)$ with midpoint $m_E := \text{mid}(E)$, the product rule for jumps $[\cdot]_E$ and averages $\langle \cdot \rangle_E$ leads to

$$\int_E [(u_{PS}^0)^2]_E \ ds = 2 \int_E [u_{PS}^0]_E \langle u_{PS}^0 \rangle_E \ ds = 2 \int_E [u_{PS}^0]_E (\langle u_{PS}^0 \rangle_E - u_{PS}^0(m_E)) ds.$$

Since $[u_{PS}^0]_E$ and $\langle u_{PS}^0 \rangle_E - u_{PS}^0(m_E)$ are affine along E and vanish in m_E,

$$2 \int_E [u_{PS}^0]_E (\langle u_{PS}^0 \rangle_E - u_{PS}^0(m_E)) ds \le \frac{h_E^3}{6} \left(|\nabla u_{PS}^0|_{Q_1}|^2 + |\nabla u_{PS}^0|_{Q_2}|^2 \right)$$

$$\le \frac{h_E \kappa}{6 \sin \omega_0} \|\nabla_{NC} u_{PS}^0\|_{L^2(Q_1 \cup Q_2)}^2.$$

In the case that Q is a triangle, the aforementioned arguments remain valid with the substitution of κ by 4. The discrete Friedrichs inequality (5.5) as well as the combination of the preceding estimates and the summation over all quadrilaterals and triangles lead to

$$\frac{1}{1+C_{\mathrm{dF}}^2}\left(\alpha_{\min} - \frac{h_{\max}\beta_{\max}\kappa}{\sin\omega_0}\right)\|u_{PS}^0\|_{H^1(\mathcal{T})}^2 \le a_{NC}(u_{PS}^0, u_{PS}^0).$$

Provided $h_{\max}$ is sufficiently small as in (5.6), this implies ellipticity in the sense of

$$\frac{\alpha_{\min}}{2+2C_{\mathrm{dF}}^2}\|u_{PS}^0\|_{H^1(\mathcal{T})}^2 \le a_{NC}(u_{PS}^0, u_{PS}^0). \qquad \square$$

Remark 5.1. With an analogous calculation, the ellipticity of $\|\!|\cdot|\!\|_{NC}$ can be shown for functions in $H_0^1(\Omega) + PS_0(\mathcal{T})$. For sufficient small $h_{\max}$ and $v \in H_0^1(\Omega) + PS_0(\mathcal{T})$, it holds that

$$(5.7) \qquad \frac{\alpha_{\min}}{2}\|\nabla_{NC}v\|_{L^2(\Omega)}^2 = \frac{\alpha_{\min}}{2}|v|_{NC}^2 \le \|\!|v|\!\|_{NC}^2.$$

5.3. Strang lemma. In the case $\mathbf{b} = 0$, $\|\!|\cdot|\!\|_{NC}$ is a norm for the space $H_0^1(\Omega) + PS_0(\mathcal{T})$. Otherwise, $\|\!|\cdot|\!\|_{NC}$ is only positive definite for sufficient fine meshes and the triangle inequality involves a constant, as shown in the following lemma.

LEMMA 5.3 (generalized triangle inequality). *Let $u, v \in H_0^1(\Omega) + PS_0(\mathcal{T})$ and the mesh-size sufficiently small such that* (5.7) *holds. Then the constants*

$$C_{\max} := (\alpha_{\max} + \beta_{\max}C_{dF} + \gamma_{\max}C_{dF}^2)/\alpha_{\min} \ and \ C_\Delta := \sqrt{C_{\max} + 1/2}$$

satisfy

$$(5.8) \qquad \|\!|u+v|\!\|_{NC} \le C_\Delta\ (\|\!|u|\!\|_{NC} + \|\!|v|\!\|_{NC}).$$

Proof. The bounds of $\mathbb{A}, \mathbf{b}$, and γ, (5.7), (5.5), and the Young inequality yield

$$\begin{aligned}
\|\!|u+v|\!\|_{NC}^2 &\le \|\!|u|\!\|_{NC}^2 + \|\!|v|\!\|_{NC}^2 + 2\alpha_{\max}|u|_{NC}|v|_{NC} \\
&\quad + \beta_{\max}(|u|_{NC}\|v\|_{L^2(\Omega)} + |v|_{NC}\|u\|_{L^2(\Omega)}) + 2\gamma_{\max}\|u\|_{L^2(\Omega)}\|v\|_{L^2(\Omega)} \\
&\le \|\!|u|\!\|_{NC}^2 + \|\!|v|\!\|_{NC}^2 + 4C_{\max}\|\!|u|\!\|_{NC}\|\!|v|\!\|_{NC} \\
&\le (C_{\max} + 1/2)(\|\!|u|\!\|_{NC} + \|\!|v|\!\|_{NC})^2. \qquad \square
\end{aligned}$$

THEOREM 5.4 (Strang lemma). *The Strang lemma for the present situation reads*

$$(5.9) \quad \begin{aligned}
\|\!|u_0 - u_{PS}^0|\!\|_{NC} &\le C_\Delta\left(\inf_{v_{PS}\in PS_0(\mathcal{T})}\|\!|u_0 - v_{PS}|\!\|_{NC}\right. \\
&\quad \left. + \sqrt{\frac{2}{\alpha_{\min}}}\sup_{w_{PS}\in PS_0(\mathcal{T})}\frac{|a_{NC}(u_0, w_{PS}) - F_{NC}(w_{PS})|}{|w_{PS}|_{NC}}\right).
\end{aligned}$$

Proof. The proof of the Strang lemma in a standard formulation (see, e.g., [BS08, Lemma 10.1.9]) uses the triangle inequality of the energy norm $\sqrt{a_{NC}(\cdot,\cdot)}$. Instead we use the generalized triangle inequality (5.8). Furthermore, Theorem 5.2 implies for $\mathbf{b}$ piecewise constant and small $h_{\max}$ as in (5.6) that

$$\alpha_{\min}/2\ |w_{PS}|_{NC}^2 \le \|\!|w_{PS}|\!\|_{NC}^2. \qquad \square$$

5.4. Approximation error. This subsection is devoted to the analysis of the approximation error

$$\inf_{v_{PS} \in PS_0(\mathcal{T})} \|\|u_0 - v_{PS}\|\|_{NC} \leq \|\|u_0 - Ju_0\|\|_{NC}$$

with the interpolation operator J from section 4 and $Ju_0 \in PS_0(\mathcal{T})$. The estimates (4.5)–(4.6) from Theorem 4.2 on quadrilaterals and (4.1)–(4.2) from Proposition 4.1 on triangles apply to $e := w - Jw$ with the assumptions on $\mathbb{A}$, $\mathbf{b}$, γ and lead to

$$\begin{aligned}
\|\|e\|\|_Q^2 :=& \int_Q \mathbb{A}\nabla e \cdot \nabla e \; dx + \int_Q (\mathbf{b} \cdot \nabla e + \gamma e)e \; dx \\
\leq& \; \alpha_{\max}\|\nabla e\|_{L^2(Q)}^2 + \beta_{\max}\|\nabla e\|_{L^2(Q)}\|e\|_{L^2(Q)} + \gamma_{\max}\|e\|_{L^2(Q)}^2 \\
\leq& \left(\alpha_{\max} \max\{C^2(\theta_0), C^2(\omega_0)\}h_Q^2 + \beta_{\max}(\sqrt{5/3}C(\omega_0) + C(\theta_0))^2 h_Q^3 \right. \\
& \left. + \gamma_{\max}(2C(\omega_0) + C(\theta_0)/2)^2 h_Q^4 \right)\|D^2 u_0\|_{L^2(Q)}^2 \\
=:& \; (C_{\text{app}}^2 + C_1^2 h_Q + C_2^2 h_Q^2) \; \|h_Q D^2 u_0\|_{L^2(Q)}^2 .
\end{aligned}$$

The constants $C(\theta_0)$ and $C(\omega_0)$ are as in Theorem 4.2. Hence,

$$(5.10) \qquad \|\|u_0 - Ju_0\|\|_{NC} \leq (C_{\text{app}} + C_1 h^{1/2} + C_2 h) \; \|h D^2 u_0\|_{L^2(\Omega)}.$$

5.5. Consistency error. This subsection is devoted to the analysis of the consistency error and is based on the calculations in [PS03] to prove

$$(5.11)$$
$$\sup_{w_{PS} \in PS_0(\mathcal{T})} \frac{|a_{NC}(u_0, w_{PS}) - F_{NC}(w_{PS})|}{|w_{PS}|_{NC}} \leq \frac{\sqrt{8}\kappa\alpha_{\max}}{\sqrt{3}\; \sin\omega_0} \left(\frac{1+\pi}{\pi^2} \right)^{1/2} \|h D^2 u\|_{L^2(\Omega)}.$$

Throughout this subsection, v_j denotes the restriction of v to a quadrilateral Q_j.

5.5.1. Projection R_0. Let $\gamma_{j,k}$ denote some interior edge common to $Q_j, Q_k \in \mathcal{T}$. Further, let $\langle \cdot, \cdot \rangle_\gamma$ denote the L^2-scalar product on γ. Set $P_0(\mathcal{E})$ the space of edgewise constant functions and define the projection

$$R_0 : H^2(\Omega) \to P_0(\mathcal{E})$$

by

$$\langle \nu_j \cdot \mathbb{A}\nabla v_j - R_0 v_j, z \rangle_\gamma = 0$$

for all $z \in P_0(\gamma)$, where γ equals either an interior edge $\gamma_{j,k}$ or an boundary edge. This requires $\mathbb{A}\nabla v \in H(\text{div},\Omega) \cap L^{2+\epsilon}(\Omega)$ for some $\epsilon > 0$, which is the case for the exact solution u. The paper [PS03] shows for adjacent quadrilaterals or triangles $Q_j, Q_k \in \mathcal{T}$ and $w_{PS} \in PS(\mathcal{T})$ the orthogonality

$$(5.12) \qquad \langle R_0 v_j, w_{PS}|_{Q_j} \rangle_{\gamma_{j,k}} + \langle R_0 v_k, w_{PS}|_{Q_k} \rangle_{\gamma_{j,k}} = 0.$$
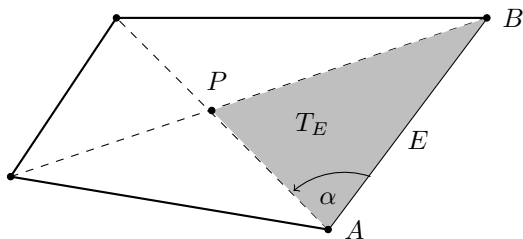
FIG. 5.1. *Quadrilateral Q divided into four subtriangles. T_E denotes the triangle with edge E.*

5.5.2. Estimate of $\|\boldsymbol{\nu}|_Q \cdot \mathbb{A}\boldsymbol{\nabla u}|_Q - \boldsymbol{R_0 u}|_Q\|_{\boldsymbol{L^2(\partial Q)}}$. To shorten the notation, set

$$g_Q := \nu|_Q \cdot \mathbb{A}\nabla u|_Q \in L^2(\partial Q) \text{ and } g_{Q,E} := \nu|_E \cdot \mathbb{A}\nabla u|_Q \in L^2(E).$$

Then $R_0 u|_Q$ is the edgewise integral mean of g_Q along the boundary of Q. Consider the decomposition of Q into four triangles as in Figure 5.1 and let $\overline{g}_{Q,E}$ denote the integral mean of $g_{Q,E}$ on T_E.

LEMMA 5.5 (trace inequality I). *Let Q be a quadrilateral with diameter h_Q and shape regularity constants ω_0 and κ, which is divided into four triangles as in Figure 5.1. Let E denote some edge of Q with neighboring triangle T_E. Let $f \in H^1(T_E)$ satisfy $\int_{T_E} f(x)dx = 0$. Then,*

$$(5.13) \qquad \|f\|_{L^2(E)}^2 \leq \frac{8\kappa}{\sin \omega_0} \left(\frac{1}{\pi^2} + \frac{1}{\pi} \right) h_Q \|\nabla f\|_{L^2(T_E)}^2.$$

Proof. The trace identity (4.3) leads directly to a trace inequality on T_E. Together with the Poincaré inequality, this implies

$$\|f\|_{L^2(E)}^2 \leq \frac{|E|}{|T_E|}\|f\|_{L^2(T_E)}(\|f\|_{L^2(T_E)} + h_{T_E}\|\nabla f\|_{L^2(T_E)})$$
$$\leq \frac{|E|}{|T_E|}h_{T_E}^2 \left(\frac{1}{\pi^2} + \frac{1}{\pi} \right) \|\nabla f\|_{L^2(T_E)}^2.$$

Shape regularity shows for $\alpha := \angle BAP$ from Figure 5.1 the estimate $\sin \omega_0/(2\kappa) \leq \sin \alpha$. Then $|T_E| = (|E||\overline{AP}| \sin \alpha)/2$ concludes the proof. $\quad\square$

This subsubsection concludes with an application of Lemma 5.5 to control $\|\nu|_Q \cdot \mathbb{A}\nabla u|_Q - R_0 u|_Q\|_{L^2(\partial Q)}$. The Pythagoras theorem implies $\|g_Q - R_0 u|_Q\|_{L^2(E)} \leq \|g_Q - \overline{g}_{Q,E}\|_{L^2(E)}$. Therefore,

$$\begin{aligned}
\|g_Q - R_0 u|_Q\|_{L^2(\partial Q)}^2 &\leq \sum_{E \in \partial Q} \|g_{Q,E} - \overline{g}_{Q,E}\|_{L^2(E)}^2 \\
&\overset{(5.13)}{\leq} C_{\mathrm{tr}}\, h_Q \sum_{E \in \partial Q} \|\nabla g_{Q,E}\|_{L^2(T_E)}^2 \\
(5.14) \qquad &\leq C_{\mathrm{tr}}\, \alpha_{\max}^2 h_Q \|D^2 u\|_{L^2(Q)}^2.
\end{aligned}$$

For a quadrilateral Q, $C_{\mathrm{tr}} := 8\kappa/\sin \omega_0 (1/\pi^2 + 1/\pi)$ from Lemma 5.5. For a triangle set $T_E := Q$ and substitute κ by 1.

5.5.3. Estimate of $|a_{NC}(u_0, w_{PS}) - F_{NC}(w_{PS})|$. Let $w_{PS} \in PS_0(\mathcal{T})$ be arbitrary. An integration by parts leads with (5.1) to

$$a_{NC}(u_0, w_{PS}) - F_{NC}(w_{PS})$$

$$= \sum_{j=1}^{|\mathcal{T}|} \left(\int_{Q_j} (\mathbb{A}\nabla u) \cdot \nabla w_{PS} \; dx + \int_{Q_j} (\mathbf{b} \cdot \nabla u + \gamma u) w_{PS} \; dx \right) - \int_\Omega f w_{PS} \; dx$$

$$\stackrel{(5.1)}{=} \sum_{j=1}^{|\mathcal{T}|} \int_{\partial Q_j} w_{PS} \; (\nu_j \cdot \mathbb{A}\nabla u) \; ds$$

$$\stackrel{(5.12)}{=} \sum_{j=1}^{|\mathcal{T}|} \langle \nu_j \cdot \mathbb{A}\nabla u_j - R_0 u_j, \; w_{PS}|_{Q_j} \rangle_{\partial Q_j}$$

$$= \sum_{j=1}^{|\mathcal{T}|} \langle \nu_j \cdot \mathbb{A}\nabla u_j - R_0 u_j, \; w_{PS}|_{Q_j} - m_j \rangle_{\partial Q_j}.$$

This holds for any edgewise constant m_j, which is set as the integral mean

$$m_j|_E := \fint_E w_{PS}|_{Q_j} \; ds.$$

The Cauchy–Schwarz inequality leads to

$$|a_{NC}(u_0, w_{PS}) - F_{NC}(w_{PS})|$$

$$\leq \left| \sum_{j=1}^{|\mathcal{T}|} h_{Q_j}^{1/2} \| \nu_j \cdot \mathbb{A}\nabla u_j - R_0 u_j \|_{L^2(\partial Q_j)} \; h_{Q_j}^{-1/2} \| w_{PS}|_{Q_j} - m_j \|_{L^2(\partial Q_j)} \right|$$

$$\leq \underbrace{\left(\sum_{j=1}^{|\mathcal{T}|} h_{Q_j} \| \nu_j \cdot \mathbb{A}\nabla u_j - R_0 u_j \|_{L^2(\partial Q_j)}^2 \right)^{1/2}}_{(*)} \underbrace{\left(\sum_{j=1}^{|\mathcal{T}|} h_{Q_j}^{-1} \| w_{PS} - m_j \|_{L^2(\partial Q_j)}^2 \right)^{1/2}}_{(**)}.$$

Estimate (5.14) allows for

$$(*) \leq \frac{8\kappa \; \alpha_{\max}^2}{\sin \omega_0} \left(\frac{1}{\pi^2} + \frac{1}{\pi} \right) \| h D^2 u \|_{L^2(\Omega)}^2.$$

The subsequent lemma allows for the control of $(**)$.

LEMMA 5.6 (trace inequality II). *Let Q be a quadrilateral or triangle with diameter h_Q and shape regularity constants ω_0 and κ. Let $w \in P_1(Q)$ be affine with integral mean $m|_E := \fint_E w \; ds$ along any edge $E \in \mathcal{E}(Q)$. Then it holds that*

$$\| w - m \|_{L^2(\partial Q)}^2 \leq \frac{\kappa}{3 \sin \omega_0} h_Q \| \nabla w \|_{L^2(Q)}^2.$$

Proof. Since ∇w is constant on Q, it holds that

$$\|w - m\|^2_{L^2(\partial Q)} = \sum_{E \in \mathcal{E}(Q)} \int_E |x - \mathrm{mid}(E)|^2 \left(\frac{\partial w}{\partial s}\right)^2 ds$$

$$\leq \frac{1}{12} \max_{E \in \mathcal{E}(Q)} h_E^2 \, \|\nabla w\|^2_{L^2(\partial Q)}$$

$$= \frac{1}{12} \max_{E \in \mathcal{E}(Q)} h_E^2 \, \frac{|\partial Q|}{|Q|} \|\nabla w\|^2_{L^2(Q)}.$$

Shape regularity results in

$$\max_{E \in \mathcal{E}(Q)} h_E \, |\partial Q| \leq 4\kappa \frac{|Q|}{\sin \omega_0}. \qquad \square$$

Lemma 5.6 implies

$$(**) \leq \sum_j \frac{\kappa}{3 \sin \omega_0} \|\nabla w_{PS}\|^2_{L^2(Q_j)} = \frac{\kappa}{3 \sin \omega_0} |w_{PS}|^2_{NC}.$$

The combination of the aforementioned estimates of $(*)$–$(**)$ verifies

$$|a_{NC}(u_0, w_{PS}) - F_{NC}(w_{PS})| \leq \frac{\sqrt{8}\kappa \alpha_{\max}}{\sqrt{3} \, \sin \omega_0} \left(\frac{1 + \pi}{\pi^2}\right)^{1/2} \|h D^2 u\|_{L^2(\Omega)} \, |w_{PS}|_{NC}.$$

Since $w_{PS} \in PS_0(\mathcal{T})$ is arbitrary, this proves (5.11).

5.6. Result. In the case $\mathbf{b} \neq 0$ and $\mathbf{b}$ piecewise constant, we consider $h_{\max}$ to be as small as in (5.6). Then, the Strang lemma (5.9), the approximation error (5.10), and the consistency error (5.11) lead to the a priori estimate

$$\|u_0 - u_{PS}^0\|_{NC} \leq C_\Delta (C_{\mathrm{app}} \|h D^2 u_0\|_{L^2(\Omega)} + C_{\mathrm{con}} \|h D^2 u\|_{L^2(\Omega)}$$
$$+ (C_1 h^{1/2} + C_2 h) \|h D^2 u_0\|_{L^2(\Omega)}).$$

The constant C_Δ is from Lemma 5.3, while $C_{\mathrm{app}}, C_1, C_2$ are from section 5.4 and

$$C_{\mathrm{con}} := \frac{4\kappa \, \alpha_{\max}}{\sqrt{3}\alpha_{\min} \, \sin \omega_0} \left(\frac{1 + \pi}{\pi^2}\right)^{1/2}.$$

The rest of this section is devoted to the discussion of $\|u - u_{PS}\|_{NC}$.

Approximation of Dirichlet boundary conditions. From section 5.4 we obtain the constants for estimates of the form $\|u_D - Ju_D\|_{L^2(\Omega)} \lesssim \|h^2 D^2 u_D\|_{L^2(\Omega)}$, $\|\nabla_{NC}(u_D - Ju_D)\|_{L^2(\Omega)} \lesssim \|h D^2 u_D\|_{L^2(\Omega)}$ as well as

$$\|u_D - Ju_D\|_{NC} \leq (C_{\mathrm{app}} + C_1 h^{1/2} + C_2 h) \|h D^2 u_D\|_{L^2(\Omega)}.$$

Approximation of lower-order terms. The discrete Friedrichs inequality (5.5) yields a bound of $u_0 - u_{PS}^0$ in the L^2-norm,

$$\|u_0 - u_{PS}^0\|_{L^2(\Omega)} \leq C_{\mathrm{dF}} \|\nabla_{NC}(u_0 - u_{PS}^0)\|_{L^2(\Omega)} =: C_{\mathrm{dF}} |u_0 - u_{PS}^0|_{NC}.$$

To bound the error in the H^1-seminorm, let $\tilde{u}_0 \in PS_0(\mathcal{T})$ denote the best approximation of u_0 in $PS_0(\mathcal{T})$. Then, (5.7) implies

$$\|\nabla_{NC}(u_0 - u_{PS}^0)\|_{L^2(\Omega)} \leq \|\nabla_{NC}(u_0 - \tilde{u}_0)\|_{L^2(\Omega)} + \|\nabla_{NC}(u_{PS}^0 - \tilde{u}_0)\|_{L^2(\Omega)}$$

$$\leq \|\nabla_{NC}(u_0 - Ju_0)\|_{L^2(\Omega)} + \sqrt{\frac{2}{\alpha_{\min}}} \, \|\|u_{PS}^0 - \tilde{u}_0\|\|_{NC}.$$

The best-approximation property of $\tilde{u}_0$ leads to

$$\|\|u_{PS}^0 - \tilde{u}_0\|\|_{NC}^2 = a_{NC}(u_{PS}^0 - u_0, u_{PS}^0 - \tilde{u}_0) = F_{NC}(u_{PS}^0 - \tilde{u}_0) - a_{NC}(u_0, u_{PS}^0 - \tilde{u}_0),$$

i.e., the consistency error from section 5.5. This results in

$$\|\nabla_{NC}(u_0 - u_{PS}^0)\|_{L^2(\Omega)} \leq \frac{C_{\text{app}}}{\sqrt{\alpha_{\max}}}\|hD^2 u_0\|_{L^2(\Omega)} + C_{\text{con}}\|hD^2 u\|_{L^2(\Omega)}.$$

Estimation of complete error. Recall that the triangle inequality is not valid for $\|\| \cdot \|\|_{NC}$. Also, the generalized triangle inequality from Lemma 5.3 cannot be used to combine the two estimates since $u_D \notin H_0^1(\Omega) + PS_0(\mathcal{T})$. Nevertheless,

$$\|\|u - u_{PS}\|\|_{NC}^2 = \|\|u_D - Ju_D\|\|_{NC}^2 + \|\|u_0 - u_{PS}^0\|\|_{NC}^2$$
$$+ a_{NC}(u_D - Ju_D, u_0 - u_{PS}^0) + a_{NC}(u_0 - u_{PS}^0, u_D - Ju_D)$$
$$\leq \|\|u_D - Ju_D\|\|_{NC}^2 + \|\|u_0 - u_{PS}^0\|\|_{NC}^2$$
$$+ 2\alpha_{\max}|u_D - Ju_D|_{NC}|u_0 - u_{PS}^0|_{NC}$$
$$+ \beta_{\max}(|u_D - Ju_D|_{NC}\|u_0 - u_{PS}^0\|_{L^2(\Omega)}$$
$$+ |u_0 - u_{PS}^0|_{NC}\|u_D - Ju_D\|_{L^2(\Omega)})$$
$$+ 2\gamma_{\max}\|u_D - Ju_D\|_{L^2(\Omega)}\|u_0 - u_{PS}^0\|_{L^2(\Omega)}.$$

The combined calculations from above result in an a priori estimate with explicit constants of the form

$$\|\|u - u_{PS}\|\|_{NC} \lesssim \|hD^2 u\|_{L^2(\Omega)} + \|hD^2 u_D\|_{L^2(\Omega)} + \|hD^2 u_0\|_{L^2(\Omega)}.$$

Remark 5.2 (example from the introduction). Consider the homogeneous Poisson model problem (1.1) from the introduction with a uniform triangulation of $\Omega = (0,1)^2$ into squares and right isosceles triangles of size h. This gives in particular $\alpha_{\min} = \alpha_{\max} = 1, \beta_{\max} = 0, \gamma_{\max} = 0, \kappa = 1, \omega_0 = \theta_0 = \pi/2$. Thus, the approximation error and the consistency error involve the constants

$$C_{\text{app}} = C(\pi/2) \leq 0.68, \qquad C_{\text{con}} = 4/\pi \ \sqrt{(1+\pi)/3} \leq 1.5.$$

Because of $\mathbf{b} = \mathbf{0}$, we can use the Strang lemma in its standard formulation and obtain together with the convexity of Ω,

$$\|\|u - u_{PS}\|\|_{NC} \leq (C_{\text{app}} + C_{\text{con}}/\sqrt{2})h \ \|D^2 u\|_{L^2(\Omega)} \leq 1.75h \ \|f\|_{L^2(\Omega)}.$$

6. Numerical experiment. The computer experiment of this section is beyond the analysis of this paper in that the exact solution does not belong to $H^2(\Omega)$ and the anisotropic mesh-refinement leads to degenerate constants as $\kappa \to \infty$. Nevertheless, numerical evidence underlines that adaptivity and even anisotropy improve the convergence rate significantly. Consider the Dirichlet problem

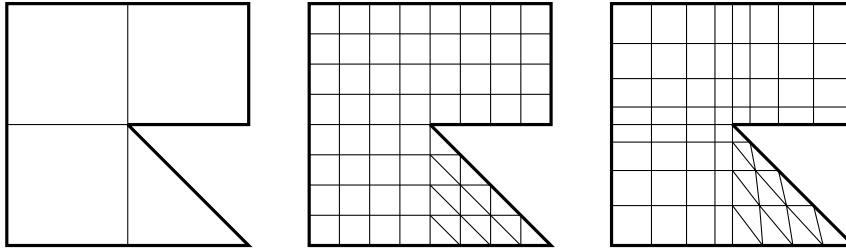$$-\Delta u = 0 \text{ in } \Omega \quad \text{and} \quad u = u_D \text{ on } \partial\Omega$$

FIG. 6.1. *Triangulations of a Z-shape domain: (left) $\mathcal{T}_0$, (middle) uniform refined mesh, and (right) graded mesh.*
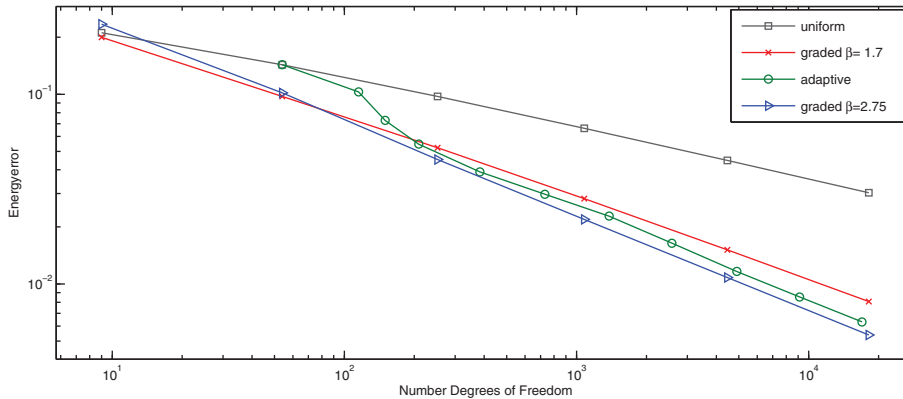

FIG. 6.2. *Plot of the energy error for uniform, graded, and adaptive refinement strategies.*

on the Z-shape $\Omega := \{x \in (-1,1)^2 |\ 0 < \arg x < 7\pi/4\}$ from Figure 6.1. In polar coordinates the exact solution and its trace $u_D = u|_{\partial\Omega}$ read

$$u(r,\varphi) = r^{4/7}\sin(4\varphi/7)$$

with a typical corner singularity at the origin. The interpolation error estimate of Theorem 4.2 leads to linear convergence for all element domains with positive distance to the reentering corner at the origin. A standard argument for the singular part of the solution leads to the interpolation estimate

$$\|u - Ju\|_{L^2(Q)} \lesssim h_Q^{4/7}.$$

It is expected that the overall final error estimate for this singular solution leads to

$$\|u - u_{PS}\|_{NC} \lesssim h_{\max}^{4/7}.$$

This is in fact observed in the numerical experiment for uniform mesh-refinement which results in an empirical convergence rate $0.28 \approx \frac{1}{2}\ 4/7$ (two space dimensions); see Figure 6.2. Graded meshes generate anisotropic elements and refine the mesh near the origin; see the right side of Figure 6.1. A graded mesh of a unit square into $(N-1)^2$ rectangles is characterized by the sequence $0, (\frac{1}{N})^\beta, (\frac{2}{N})^\beta, \ldots, 1$ with parameter $\beta \geq 1$.

The error in the energy norm of the discrete solution using Park–Sheen elements with graded meshes results in the empirical convergence rate 0.44 for $\beta = 1.7$ and

0.49 for $\beta = 2.75$; cf. Figure 6.2. Also, the adaptive algorithm gains the convergence rate 0.49, which is near the optimal convergence rate of 0.5 for first-order methods. The marking strategy involves the purely heuristic (but optimal for Crouzeix–Raviart elements [Rab10]) estimator

$$\eta^2(Q) := \sum_{E \in \mathcal{E}(Q)} h_E \, \|[\partial u_{PS}/\partial s]_E\|^2_{L^2(E)}$$

with jump $[\cdot]_E$. The marking process uses the Dörfler criterion [Dör96] and marks a minimal number of elements $\mathcal{M} \subset \mathcal{T}$ such that

$$\eta(\mathcal{M}) := \left(\sum_{Q \in \mathcal{M}} \eta^2(Q) \right)^{1/2} \geq \frac{1}{4} \eta(\mathcal{T}).$$

The adaptive finite element cycle then reads SOLVE $\rightarrow$ ESTIMATE $\rightarrow$ MARK $\rightarrow$ REFINE.

Remark 6.1 (smooth solutions). Unreported numerical examples for smooth solutions show the optimal convergence rates with (almost) quasi-uniform meshes in agreement with the theoretical results of this paper.

REFERENCES

[BM08]   R. BECKER AND S. MAO, *An optimally convergent adaptive mixed finite element method*, Numer. Math., 111 (2008), pp. 35–54.

[BS08]   S. C. BRENNER AND L. R. SCOTT, *The Mathematical Theory of Finite Element Methods*, Texts in Appl. Math. 15, 3rd ed., Springer, New York, 2008.

[CGR11] C. CARSTENSEN, J. GEDICKE, AND D. RIM, *Explicit error estimates for Courant, Crouzeix-Raviart and Raviart-Thomas finite element methods*, J. Comput. Math., submitted, 2011.

[Cia78] P. G. CIARLET, *The Finite Element Method for Elliptic Problems*, North-Holland, Amsterdam, 1978.

[CR73]   M. CROUZEIX AND P.-A. RAVIART, *Conforming and nonconforming finite element methods for solving the stationary Stokes equations*, Math. Anal. Numer., 7 (1973), pp. 33–76.

[Dör96] W. DÖRFLER, *A convergent adaptive algorithm for Poisson's equation*, SIAM J. Numer. Anal., 33 (1996), pp. 1106–1124.

[Gri85] P. GRISVARD, *Elliptic Problems in Nonsmooth Domains*, Monogr. Stud. Math. 24, Pitman, Boston, MA, 1985.

[Par03] C. PARK, *A Study on Locking Phenomena in Finite Element Computations*, Ph.D. thesis, Seoul National University, 2003.

[PS03]   C. PARK AND D. SHEEN, *P_1-nonconforming quadrilateral finite element methods for second-order elliptic problems*, SIAM J. Numer. Anal., 41 (2003), pp. 624–640.

[PW60]   L. E. PAYNE AND H. F. WEINBERGER, *An optimal Poincaré inequality for convex domains*, Arch. Ration. Mech. Anal., 5 (1960), pp. 286–292.

[Rab10] H. RABUS, *A natural adaptive nonconforming FEM of quasi-optimal complexity*, Comput. Methods Appl. Math., 10 (2010), pp. 315–325.